

Influence of Magic Angle Spinning on Sample Temperature

Arnd-Rüdiger Grimmer,^{1*} Axel Kretschmer¹ and Victoria B. Cajipe²

¹ Humboldt-Universität zu Berlin, Rudower Chaussee 5, Haus 4.1, D-12484 Berlin, Germany

² Institut des Matériaux de Nantes, 2, rue de la Houssinière, F-44072 Nantes, France

Magic angle spinning at sufficiently high rates dramatically changes the sample temperature. A method is described for calibrating a probe head for the thermal effects encountered during magic angle spinning experiments. Using $\text{Sm}_2\text{Sn}_2\text{O}_7$ as a chemical shift thermometer, the overlapping effects of 'external' heating or cooling by the bearing gas and 'internal' heating by friction on the actual sample temperature were studied. The empirical expression

$$T_s = 0.12\nu_r^2 + (3.47 - 0.013T_b)\nu_r + 0.80T_b + 58.6$$

describes the influence of the bearing gas temperature T_b (K) and the spinning rate ν_r (kHz) on the sample temperature T_s (K). © 1997 by John Wiley & Sons, Ltd.

Magn. Reson. Chem. 35, 86–90 (1997) No. of Figures: 5 No. of Tables: 1 No. of References: 14

Keywords: solid-state ^{119}Sn NMR; magic angle spinning; temperature dependence; Joule–Thomson effect; frictional heating; samarium stannate

Received 9 July 1996; revised 26 August 1996; accepted 28 August 1996

INTRODUCTION

It is well known that the use of high spinning speeds during magic angle spinning (MAS) measurements causes the rotor and the sample to heat up.^{1–6} This temperature increase is due to friction between the rotor and the bearing gas and is generally an undesirable type of sample heating. Variable-temperature (VT) MAS NMR experiments with sample temperatures different from room temperature are usually carried out by heating or cooling the bearing gas to a desired temperature. The two effects overlap in an unclear way so that when knowledge of the exact sample temperature is critical, mixing a chemical shift thermometer with the sample appears to be the ideal method. Such chemical shift thermometers have been proposed by several workers, e.g. for ^{13}C ,¹ ^{15}N ,⁷ ^{31}P ⁸ and recently for ^{207}Pb .^{9,10} MAS NMR. A comprehensive paper on the ^{119}Sn NMR of $\text{Sm}_2\text{Sn}_2\text{O}_7$ also recommended this paramagnetic material as a very sensitive high-temperature chemical shift thermometer.⁶

The technique of mixing a chemical shift thermometer with the sample is inappropriate, however, when performing VT MAS experiments on reactive and sensitive solids. We therefore decided to calibrate our probe head by systematically studying the effects of 'external' heating/cooling by the hot/cold inlet bearing gas and 'internal' heating by friction. In this paper, we present ^{119}Sn chemical shift data on $\text{Sm}_2\text{Sn}_2\text{O}_7$ which lead to

an approximate expression for the sample temperature ($250 \leq T_s \leq 340$ K) for a given MAS frequency ν_r ($0 \leq \nu_r \leq 15$ kHz) and bearing gas temperature T_b ($205 \leq T_b \leq 345$ K).

EXPERIMENTAL

Grey *et al.*⁶ found that the isotropic ^{119}Sn chemical shift δ_{iso} of paramagnetic $\text{Sm}_2\text{Sn}_2\text{O}_7$ depends on the sample temperature T_s between 190 and 349 K as follows:

$$\delta_{\text{iso}} (\text{ppm}) = -9.53 \times 10^4 [T_s (\text{K})]^{-1} + 223 \quad (1a)$$

with the slope $d\delta_{\text{iso}}/dT_s \approx 1$ (ppm K^{−1}) for $T_s \approx 300$ K. We repeated their experiments and corroborated their results in detail. During the course of the present investigations, van Moorsel *et al.*¹¹ published an improved and extended version of $\delta_{\text{iso}} = f(T_s)$ for $\text{Sm}_2\text{Sn}_2\text{O}_7$. Within the temperature interval $245 \leq T_s (\text{K}) \leq 345$, their general Eqn (8) can be rewritten as linear approximations $\delta_{\text{iso}} = f(T_s)^{-1}$ giving

$$\delta_{\text{iso}} (\text{ppm}) = -8.76 \times 10^4 [T_s (\text{K})]^{-1} + 202 \quad (1b)$$

when the first derivative was used for approximation and

$$\delta_{\text{iso}} (\text{ppm}) = -8.87 \times 10^4 [T_s (\text{K})]^{-1} + 204 \quad (1c)$$

with the Chebychev polynomial as basis of the approximation.

Both Eqns (1b) and (1c) are in sufficiently good agreement with Eqn (1a). In this work, Eqn (1a) was used for the conversion of δ_{iso} into T_s .

* Correspondence to: A.-R. Grimmer.
Contract grant sponsor: DFG.

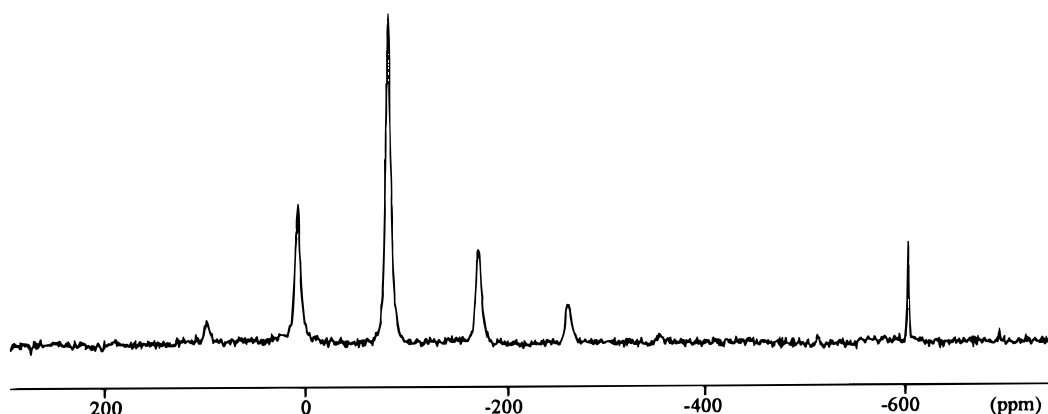


Figure 1. ^{119}Sn MAS NMR spectrum of $\text{Sm}_2\text{Sn}_2\text{O}_7$. Number of scans, 2400; 90° pulse, 2 μs ; recycle delay, 1.5 s; spinning rate, 12840 Hz; $\text{Sm}_2\text{Sn}_2\text{O}_7$ linewidth, 815 Hz; SnO_2 linewidth, 172 Hz; amount of non-reacted SnO_2 , 2.5% of total Sn.

According to Grey *et al.*,⁶ $\text{Sm}_2\text{Sn}_2\text{O}_7$ fulfils all requirements for good NMR thermometry. This stable, non-toxic compound is easily prepared from the relatively cheap oxides. Traces of non-reacted SnO_2 allow a precise *in situ* room-temperature measurement of the chemical shift relative to the ^{119}Sn isotropic chemical shift of diamagnetic SnO_2 ($\delta_{\text{iso}} = -604.3$ ppm) which serves as a secondary reference in addition to the primary standard SnMe_4 ($\delta = 0$ ppm). Owing to the short spin-lattice relaxation times ($T_1 \approx 10^{-4}$ s),⁶ typical of paramagnetic compounds, very good signal-to-noise ratios are accessible within a short time, the linewidths (full width at half-maximum) of about 800 Hz (5.6 ppm, $\nu_r \geq 2$ kHz) permitting sufficiently precise (± 0.3 ppm) measurements of the isotropic chemical shift δ_{iso} .

All ^{119}Sn MAS NMR spectra of $\text{Sm}_2\text{Sn}_2\text{O}_7$ were recorded at 142.574 MHz on a Bruker MSL 400 spectrometer using a standard Bruker MAS probe with a double-bearing rotation system. The diameter of the zirconia rotors with KelF caps was 4 mm and the bearing gas (air) pressure was adjusted to 3 bar. Note that for bearing gas temperatures below 205 K, ordinary KelF caps no longer fit the rotor owing to the different thermal expansion coefficients of zirconia and KelF. Other typical experimental parameters used were a recycle delay of 100 ms, apodization of 50 Hz and 50 scans. The bearing gas was cooled or heated, while the

drive gas was used at ambient temperature in all experiments. The bearing gas temperature was controlled by the Bruker VT unit using the probe head thermocouple. The calibration of the thermocouple was given by the internal electronics of the VT unit. The room temperature was stabilized (± 0.2 K) to suppress fluctuations that have a measurable influence on the chemical shifts. After each change of temperature, the sample was left for 10 min before recording the NMR spectrum. Even at the highest MAS spinning speeds (15 kHz) the lineshape showed no asymmetry or broadening caused by localized heating effects^{10,12,13} as found for $\text{Pb}(\text{NO}_3)_2$ with ^{207}Pb NMR linewidths of 20–25 Hz.

RESULTS

The ^{119}Sn MAS NMR spectrum of $\text{Sm}_2\text{Sn}_2\text{O}_7$ is shown in Fig. 1.

The dependence of the observed isotropic ^{119}Sn chemical shift δ_{iso} of $\text{Sm}_2\text{Sn}_2\text{O}_7$ on the rotation frequency ν_r and the bearing air temperature T_b was measured using $0 \leq \nu_r$ (kHz) ≤ 15 and $205 \leq T_b$ (K) ≤ 345 . The result was a matrix $\delta_{\text{iso}} = f(\nu_r, T_b)$ with 111 experimental points. Increasing the rotation frequency gives rise to a downfield shift of the signal, indicating an increase in sample temperature. This effect weakens at higher bearing air temperatures. The sample temperature T_s may be calculated using Eqn (1a) and plotted as a function of ν_r for various T_b as shown in Fig. 2. The results of the conversion of δ_{iso} (^{119}Sn) into sample temperature T_s by means of Eqn (1) are shown in Fig. 2.

Within experimental error (± 0.3 ppm $\approx \pm 0.3$ K), satisfactory fits to the experimental data $T_s = f(\nu_r)$ were obtained using second-order polynomials:

$$T_s = m_2 \nu_r^2 + m_1 \nu_r + m_0 \quad (2)$$

Adding higher order terms did not improve the fit significantly. An analogous square correlation ($m_1 = 0$) was observed by other workers,^{3,12} while an exponential fit² showed clearly lower reliability factors r^2 . The parameters m_2 , m_1 and m_0 , reliability factor r^2 and number of experiments n for various T_b values are given in Table 1; the corresponding curves are drawn through

Table 1. Fit parameters of the experimental data (the corresponding curves are shown in Fig. 2)

T_b (K)	m_2 (K kHz ⁻²)	m_1 (K kHz ⁻¹)	m_0 (K)	n	r^2
205	0.129	+0.922	213.4	7	0.998
250	0.121	+0.375	254.5	6	0.999
265	0.126	-0.025	270.6	7	0.999
275	0.125	+0.010	279.1	7	0.999
285	0.118	-0.143	287.7	7	0.999
295	0.115	-0.302	295.5	14	0.999
297	0.127	-0.471	298.4	7	0.999
305	0.116	-0.431	303.6	14	0.999
315	0.111	-0.507	311.6	13	0.998
325	0.112	-0.655	320.0	13	0.997
335	0.108	-0.633	327.1	9	0.987
345	0.134	-0.928	335.2	6	0.961

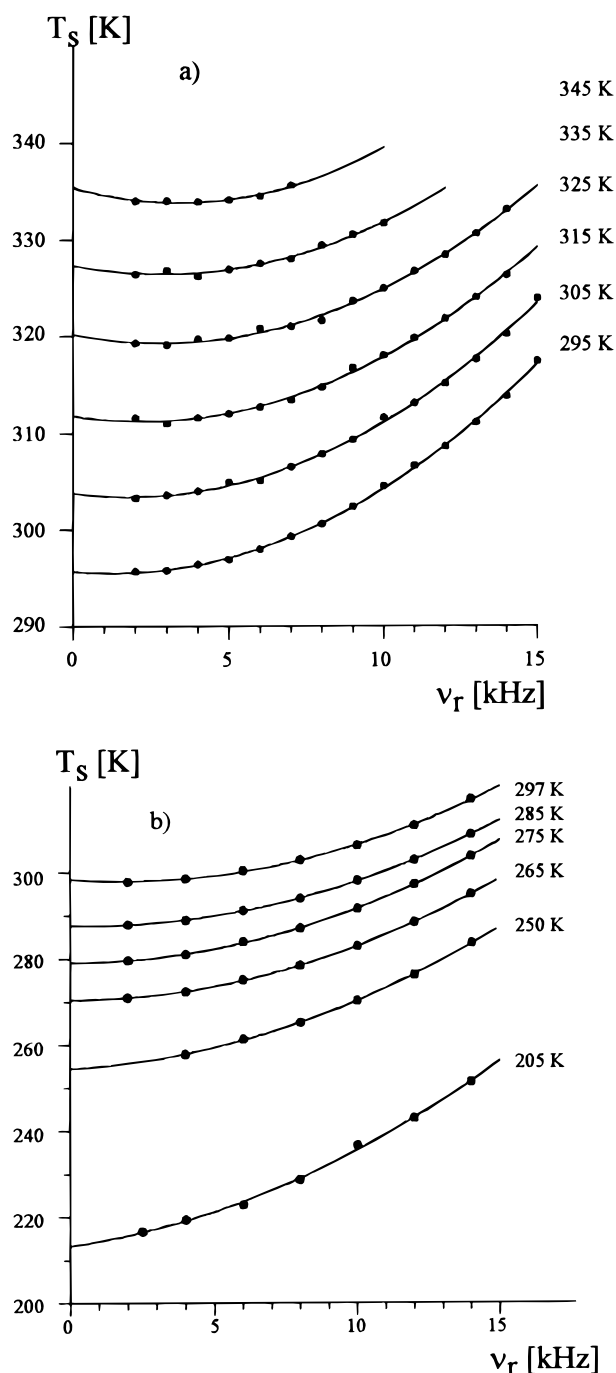


Figure 2. Sample temperature versus rotation frequency for various bearing air temperatures: (a) $T_b \geq 295$ K; (b) $T_b \leq 297$ K. Note the different T_s scales for (a) and (b).

the data points in Fig. 2(a) (T_b above room temperature) and (b) (T_b below room temperature).

DISCUSSION

The most striking feature of Fig. 2 is the strong influence of the spinning rate ν_r on the sample temperature T_s : increasing ν_r is equivalent to heating the sample. Closer inspection of the curves shows that this general statement is not valid for higher temperatures, e.g. for

$T_b = 345$ K a small but significant decrease in T_s at lower spinning rates is clearly visible. This surprising slight sample cooling was also observed by van Gorkom *et al.*¹⁰ and explained an example of the Joule–Thomson effect, which is the cooling of a real gas as it expands through a narrow aperture. At higher spinning rates the frictional heating overcomes the Joule–Thomson cooling.

Table 1 shows that the square coefficient m_2 has no significant dependence on the bearing air temperature T_b , all fits yielding practically the same value:

$$m_2 = (0.120 \pm 0.008) \text{ (K kHz}^{-2}\text{)} \quad (3)$$

except for $T_b = 335$ K and 345 K, in which case the deviation may be attributed to the smaller number of experiments. This means that the curvature is essentially identical throughout the investigated T_b range for the curves in Fig. 2.

A discussion of the physics of friction underlying this result is outside the scope of this paper. However, it should be mentioned that frictional power P_{fr} in the present case can be expressed as a product of the angular momentum L and rotation frequency squared ν_r^2 , i.e.

$$P_{fr} \text{ (W)} \approx L \nu_r^2 \text{ [(kg m}^2\text{ s}^{-1}\text{)(s}^{-2}\text{)} = \text{W}] \quad (4)$$

thus providing a qualitative explanation for the square term.¹⁴ The quantitative dependence of the Joule–Thomson cooling on ν_r is not clear, but owing to its weakness this effect is negligible.

The second (linear) coefficient m_1 clearly depends on the bearing air temperature, with increasing T_b giving rise to decreasing m_1 . Linear regression (Fig. 3) leads to

$$m_1 = -0.013 T_b + 3.47 \quad (r^2 = 0.971) \quad (5)$$

This implies that m_1 reflects the influence of T_b on T_s . Furthermore, m_1 can be used to calculate the frequency ν_r^{\min} for which T_s has its minimum, i.e. the Joule–Thomson cooling is compensated by frictional heating. Taking the first derivative of Eqn (2) and equating it to zero:

$$\frac{dT_s}{d\nu_r} = 2m_2 \nu_r + m_1 = 0 \quad (2a)$$

yields the minimum ν_r^{\min} for each $T_s = f(\nu_r)$ curve. From the data it follows that there is no cooling effect ($\nu_r^{\min} \geq 0$) for $T_b \leq 275$ K.

The third parameter, m_0 , represents the ‘static’ sample temperature. The true static sample temperature is not experimentally accessible since the large signal linewidth for a static sample precludes a sufficiently precise measurement of T_s . This observed static temperature m_0 shows an obvious deviation from the given temperature of the bearing gas T_b , the difference being ascribable to the 20 mm separation between the thermocouple and the rotating sample necessitated by the probe head construction. As expected, the temperature difference

$$\Delta = m_0 - T_b \quad (6)$$

increases with increasing deviation from room temperature ($T_b - 295$). Linear regression (Fig. 4) for

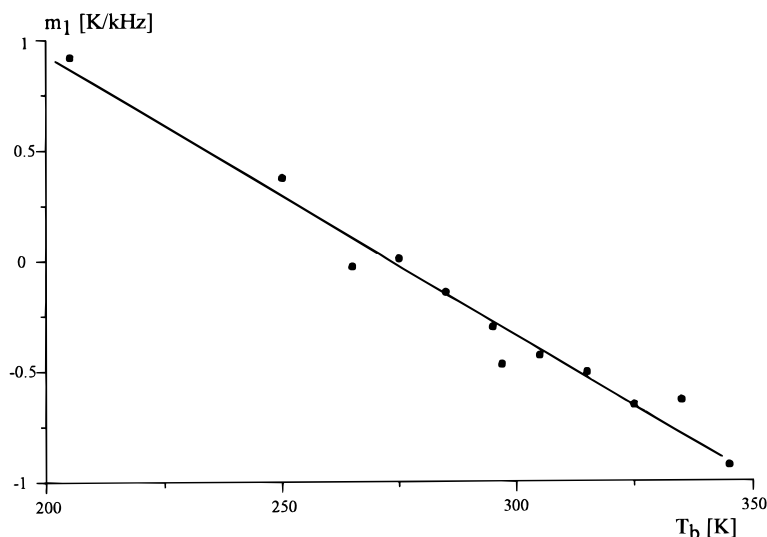


Figure 3. Linear coefficient m_1 versus bearing gas temperature.

$-30 \leq (T_b - 295) \leq 50$ K gives

$$\Delta = -0.197(T_b - 295) + 0.488 \quad (r^2 = 0.987) \quad (7)$$

i.e. Δ is about 20% of the amount that T_b is raised above room temperature. Note that the deviation of the intercept on the ordinate (*ca.* 0.5 K) from the expected value zero is of the order of the experimental error. From Eqn (7), it follows that

$$m_0 = 0.803T_b + 58.6 \quad (8)$$

The slope of Eqn (7) depends on the bearing gas pressure. The low-temperature experiments with $(T_b - 295)$ equal to -45 and -90 K were recorded with slightly elevated bearing pressure and therefore omitted for the regression. The visual extrapolation of both points gives an intercept on the abscissa of $(T_b - 295) \approx 0$, confirming this interpretation.

Combining Eqns (2), (3), (5) and (8), one obtains an expression for the sample temperature T_s (K) as a func-

tion of ν_r (kHz) and T_b (K):

$$T_s = 0.12\nu_r^2 + (3.47 - 0.013T_b)\nu_r + 0.80T_b + 58.6 \quad (9)$$

To test the validity of Eqn (9), we compared the observed and calculated sample temperatures for 32 independent and separate experiments at temperatures above room temperature. The results are summarized in Fig. 5, which also shows the straight-line fit with a slope of 1.005 and reliability factor $r^2 = 0.995$. Equation (9) thus allows an indirect determination of T_s from ν_r and T_b with an estimated error of $< \pm 1$ K and deviations increasing slightly with increasing T_s .

The experimental conditions needed to set the sample temperature at a desired value can also be calculated using Eqn (9). For example, to heat a sample to $T_s = 373$ K, a T_b of 393.0 K would be necessary in the static case, whereas in the MAS case with $\nu_r = 15$ kHz, a T_b of 389 K would be sufficient. Choosing $\nu_r = 25$ kHz, a T_b of 247 K (-26°C) would be needed to obtain the same

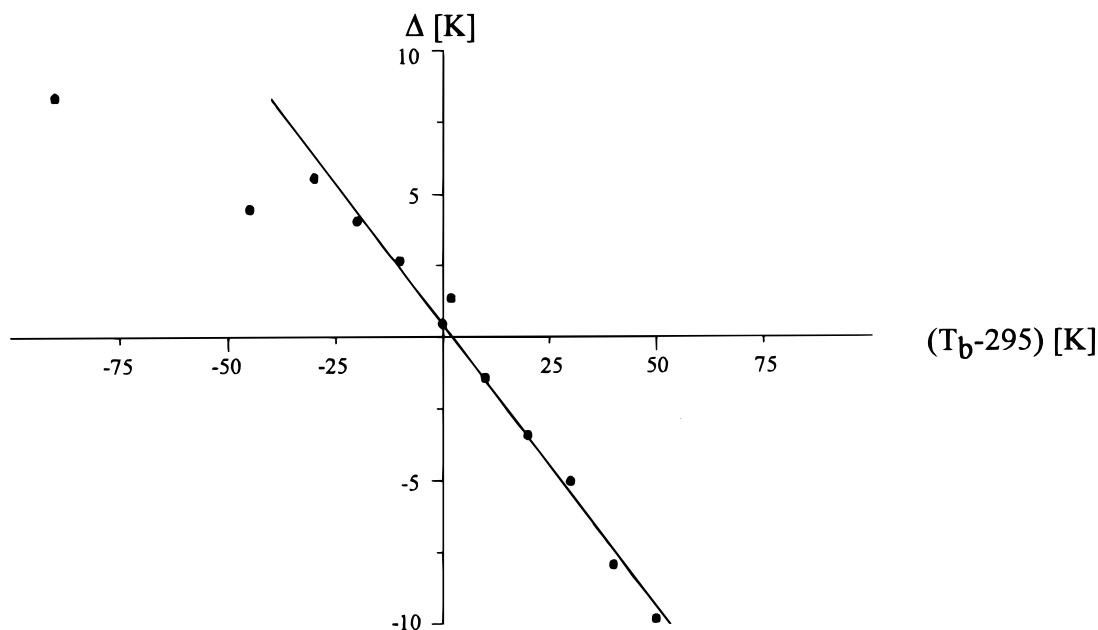


Figure 4. Temperature difference $\Delta = m_0 - T_b$ versus temperature of bearing gas.

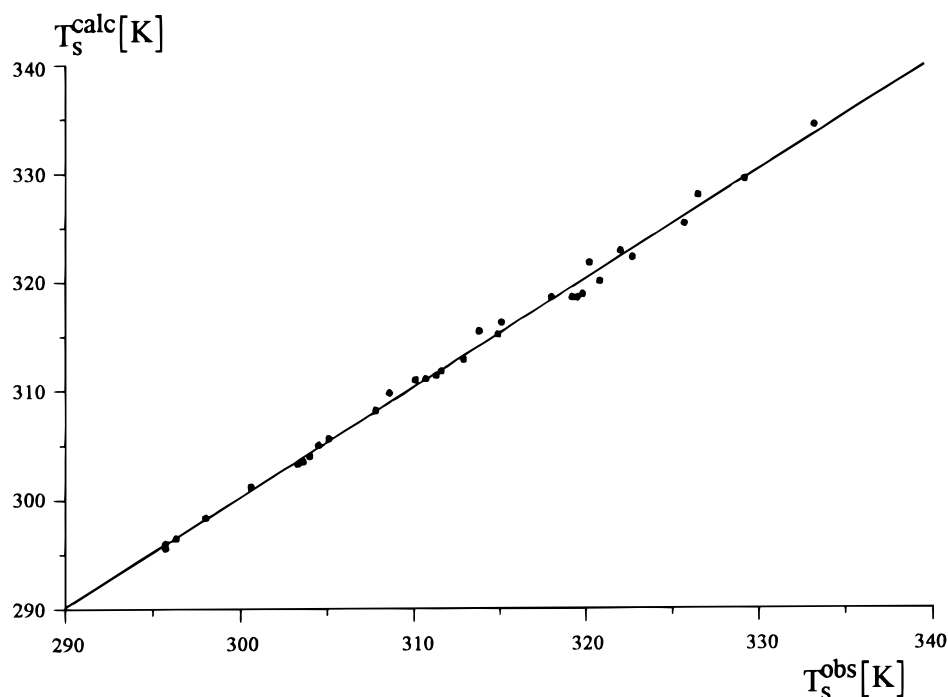


Figure 5. Observed (T_s^{obs}) versus calculated (T_s^{calc}) sample temperatures.

T_s . This latter is, however, a hypothetical case since such enormous rotation rates are not attainable using 4 mm rotors and air as a bearing gas. Finally, it should be mentioned that the coefficients in Eqn (9) generally vary with rotor material (Al_2O_3 , ZrO_2 and Si_3N_4 ¹⁰) and have to be determined from each probe head (stator). Following the procedure described above, these coefficients may be obtained within a few hours.

Qualitative experiments with a second probe head (^1H MAS) of the same type suggest the general validity of the empirical relation [Eqn (9)] derived here. The authors would be grateful for information on relevant experiments using other probes.

CONCLUSION

We have shown that in variable-temperature solid-state MAS NMR experiments the actual sample temperature

depends on the MAS spinning rate plus the bearing gas temperature. In the range 200–305 K, the superposition of simultaneous sample cooling by the Joule–Thomson effect and heating by friction results in a square dependence of a quadratic dependence of sample temperature on spinning rates. The three coefficients of the corresponding polynomial depend on the bearing gas temperature. To measure MAS spectra at constant sample temperature and increasingly higher spinning rates, the bearing gas temperature has to be reduced accordingly. For VT MAS experiments with known spinning rate and bearing gas temperature, the sample temperature can be calculated to within ± 1 K.

Acknowledgements

We are grateful to I. Busch and S. Bauer for algebraic help and to St. Steuernagel, D. Freude and K. Müller (Stuttgart) for advice and preprints. Thanks are also due to the DFG for financial support.

REFERENCES

1. G. C. Campbell, R. C. Crosby and J. F. Haw, *J. Magn. Reson.* **69**, 191 (1986).
2. T. Bjorholm and H. J. Jakobson, *J. Magn. Reson.* **84**, 204 (1989).
3. F. Aguilar-Parilla, B. Wehrle, H. Bräunling and H.-H. Limbach, *J. Magn. Reson.* **87**, 592 (1990).
4. K. L. Anderson-Altmann and D. M. Grant, *J. Phys. Chem.* **97**, 11096 (1993).
5. K. R. Morgan, S. Collier, G. Burus and K. Ooi, *J. Chem. Soc., Chem. Commun.* 1719 (1994).
6. C. P. Grey, A. K. Cheetham and Ch. M. Dobson, *J. Magn. Reson.* **A101**, 259 (1993).
7. B. Wehrle, F. Anguilar-Parilla and H.-H. Limbach, *J. Magn. Reson.* **87**, 584 (1990).
8. H. Pan and B. C. Gerstein, *J. Magn. Reson.* **92**, 618 (1991).
9. A. Bielecki and D. P. Burum, *J. Magn. Reson.* **A116**, 215 (1995).
10. L. van Gorkom, J. M. Hook, M. B. Logan, J. V. Hanna and R. E. Wasylshen, *Magn. Reson. Chem.* **33**, 791 (1995).
11. G.-J. van Moorsel, E. R. van Eck and C. P. Grey, *J. Magn. Reson.* **113**, 159 (1995).
12. T. Mildner, H. Ernst and D. Freude, *Solid State NMR* **5**, 269 (1995).
13. A. Sebald, in *NMR: Basic Principles and Progress*, edited by B. Blümlich, Vol. 31, p. 91 (1994).
14. F. P. Bowden, *Proc. R. Soc. London, Ser. A* **212**, 440 (1952).